AGU PUBLICATIONS

Geophysical Research Letters

RESEARCH LETTER
10.1002/2015GL063778

Key Points:
- Geologic and habitat characterization of a methane seep offshore southern CA
- Localized fluid flow controlled by restraining bend in San Diego Trough Fault
- Fault segment boundary role in fluid flow in strike-slip fault zones

Correspondence to:
J. M. Maloney,
jmaloney@mail.sdsu.edu

Citation:
Maloney, J. M., B. M. Grupe, A. L. Pasulka, K. S. Dawson, D. H. Case, C. A. Frieder, L. A. Levin, and N. W. Driscoll (2015), Transpressional segment boundaries in strike-slip fault systems offshore southern California: Implications for fluid expulsion and cold seep habitats, *Geophys. Res. Lett.*, *42*, 4080–4088, doi:10.1002/2015GL063778.

Received 13 MAR 2015
Accepted 1 MAY 2015
Accepted article online 5 MAY 2015
Published online 26 MAY 2015
Corrected 15 JUN 2015

This article was corrected on 15 JUN 2015. See the end of the full text for details.

Transpressional segment boundaries in strike-slip fault systems offshore southern California: Implications for fluid expulsion and cold seep habitats

Jillian M. Maloney[1,2], Benjamin M. Grupe[1,3], Alexis L. Pasulka[1,4], Katherine S. Dawson[4], David H. Case[4], Christina A. Frieder[1,5], Lisa A. Levin[1], and Neal W. Driscoll[1]

[1]Scripps Institution of Oceanography, University of California, San Diego, La Jolla, California, USA, [2]Now at Department of Geological Sciences, San Diego State University, San Diego, California, USA, [3]Now at Department of Environmental and Ocean Sciences, University of San Diego, San Diego, California, USA, [4]Division of Geological and Planetary Sciences, California Institute of Technology, Pasadena, California, USA, [5]Now at Department of Biological Sciences, University of Southern California, Los Angeles, California, USA

Abstract The importance of tectonics and fluid flow in controlling cold seep habitats has long been appreciated at convergent margins but remains poorly understood in strike-slip systems. Here we present geophysical, geochemical, and biological data from an active methane seep offshore from Del Mar, California, in the inner California borderlands (ICB). The location of this seep appears controlled by localized transpression associated with a step in the San Diego Trough fault zone and provides an opportunity to examine the interplay between fluid expulsion and restraining step overs along strike-slip fault systems. These segment boundaries may have important controls on seep locations in the ICB and other margins characterized by strike-slip faulting (e.g., Greece, Sea of Marmara, and Caribbean). The strike-slip fault systems offshore southern California appear to have a limited distribution of seep sites compared to a wider distribution at convergent plate boundaries, which may influence seep habitat diversity and connectivity.

1. Introduction

Cold seeps have been recognized on both passive and active continental margins [e.g., *Paull et al.*, 1985; *Hovland and Judd*, 1988; *Silver et al.*, 2000; *Boetius and Wenzhofer*, 2013]. Cold seeps located in the deep sea along these margins provide the foundation for diverse chemosynthetic ecosystems, which can contain more biomass and utilize more oxygen than the surrounding deep-sea communities by orders of magnitude [*Levin*, 2005; *Boetius and Wenzhofer*, 2013]. The controls on fluid seepage at convergent margins are fairly well understood [e.g., *Le Pichon et al.*, 1992; *Moore and Vrolijk*, 1992; *Carson and Screaton*, 1998]. In subduction settings, oceanic sediments from the subducted slab are extensively compressed and deformed. Extensive compaction of sediments within the wedge leads to increased pore fluid pressure and dispersed flow, with fluid expulsion along faults, mud volcanoes, and diapirs. Both shallow biogenic and deep thermogenic sources of methane are observed at subduction margins [*Moore and Vrolijk*, 1992], and numerous cold seep ecosystems have been identified and studied in these settings [e.g., *Kulm et al.*, 1986; *Sahling et al.*, 2002; *Levin and Mendoza*, 2007; *Levin et al.*, 2010]. Seeps have also been identified along strike-slip margins, but controls on fluid seepage in these tectonic settings are less well understood [*Zitter et al.*, 2008; *Geli et al.*, 2008; *Tryon et al.*, 2012], and the role of fault segment boundaries in controlling seep distribution has yet to be fully examined. Here we present data from a recently discovered seep located at a fault segment boundary within the strike-slip margin offshore southern California. Other methane seeps have previously been identified in this region that appear to be tectonically controlled [e.g., *Lonsdale*, 1979; *Torres et al.*, 2002; *Hein et al.*, 2006; *Paull et al.*, 2008], but a pattern of distribution related to the strike-slip system has not been identified. The newly discovered seep provides an ideal opportunity to examine the role of localized fault segment boundaries on fluid expulsion and the implications for regional ecology.

The geomorphic province offshore southern California is known as the inner California borderlands (ICB) and is characterized by a system of basins and ridges, and extensive strike-slip faulting (Figure 1a). The ICB may accommodate up to ~20% of the ~50 mm/yr right-lateral motion between the Pacific and North American

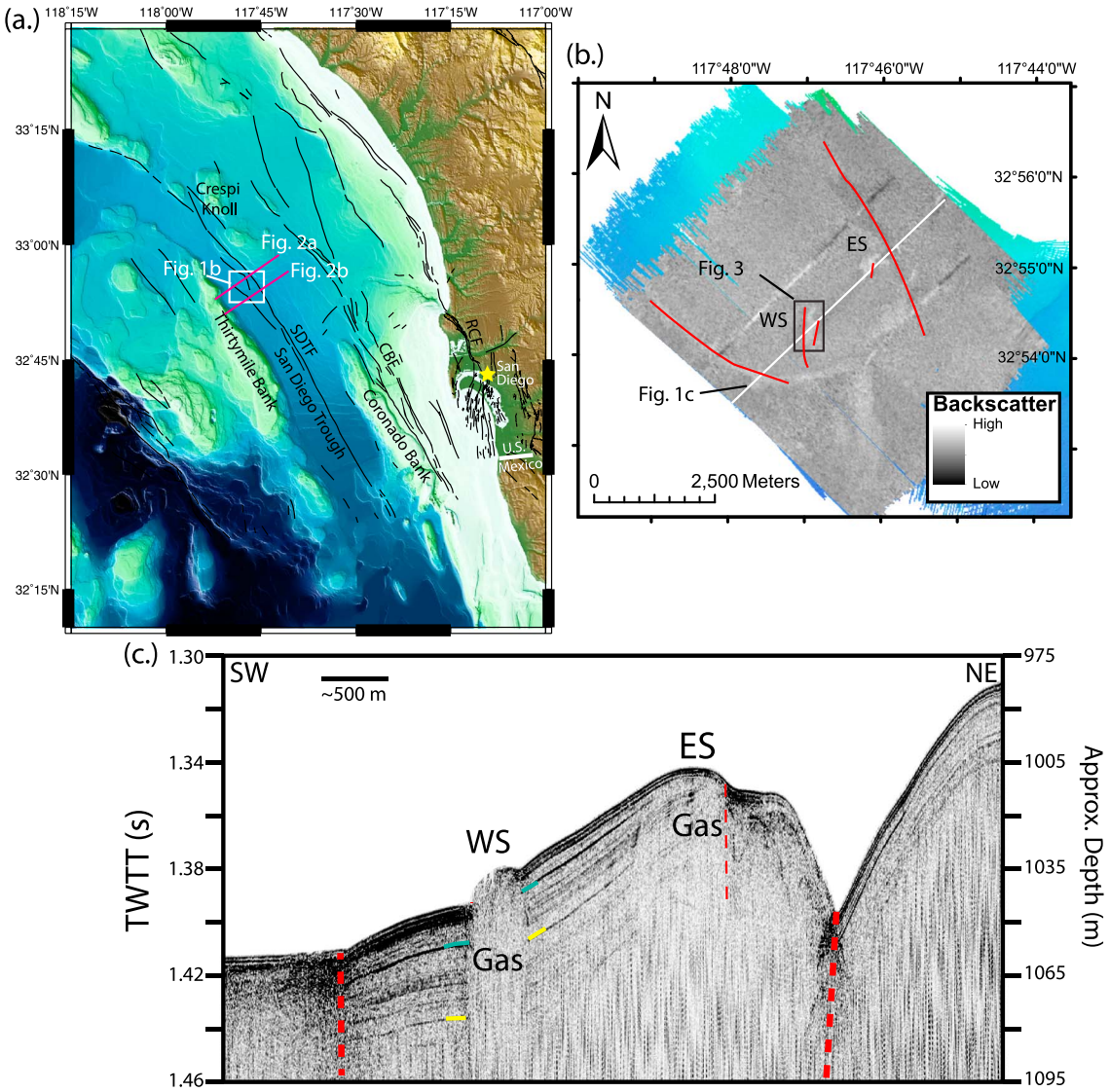

Figure 1. (a) Regional map of the inner California borderlands with major fault zones shown in black [*U.S. Geological Survey*, 2006]. Red lines show location of multichannel seismic (MCS) profiles in Figure 2. White box outlines area shown in Figure 1b. (b) Acoustic backscatter over the Del Mar Seep area showing high backscatter zones at the western region (WS) and eastern region (ES). High backscatter is light. Red lines are faults mapped in the Chirp data. The white line corresponds to the Chirp profile shown in Figure 1c. (c) Chirp profile across WS and ES, which are imaged as areas of acoustic wipeout. Offset of acoustic horizons across the WS increase with depth as illustrated by blue and yellow marked horizons (faults on either side of the WS mapped in Figure 1b are not drawn in the profile to highlight the offset horizons better). RCF = Rose Canyon Fault; CBF = Coronado Bank Fault; SDTF = San Diego Trough Fault.

Plates [*Bennett et al*., 1996; *Becker et al*., 2005; *Meade and Hager*, 2005]. The San Diego Trough is a major basin within the ICB (Figure 1a). *Ryan et al*. [2012] identified a contractional pop-up structure in the northern San Diego Trough, as well as two small rough areas indicative of fluid seepage in bathymetry data over the pop-up. We investigated this pop-up structure located at a restraining step over in the San Diego Trough fault (SDTF), south of Crespi Knoll, with geophysical mapping, remotely operated vehicle (ROV) surveys, and sediment sampling, and discovered an active methane seep (Del Mar Seep) (Figure 1a). Here we present these data and investigate the importance of strike-slip segment boundaries on seep distribution in the ICB.

2. Methods

Data were collected during two cruise efforts aboard the R/V *Melville* in July (MV1209) and December 2012 (MV1217). Multibeam and backscatter data were collected with the hull-mounted Kongsberg EM122 at a

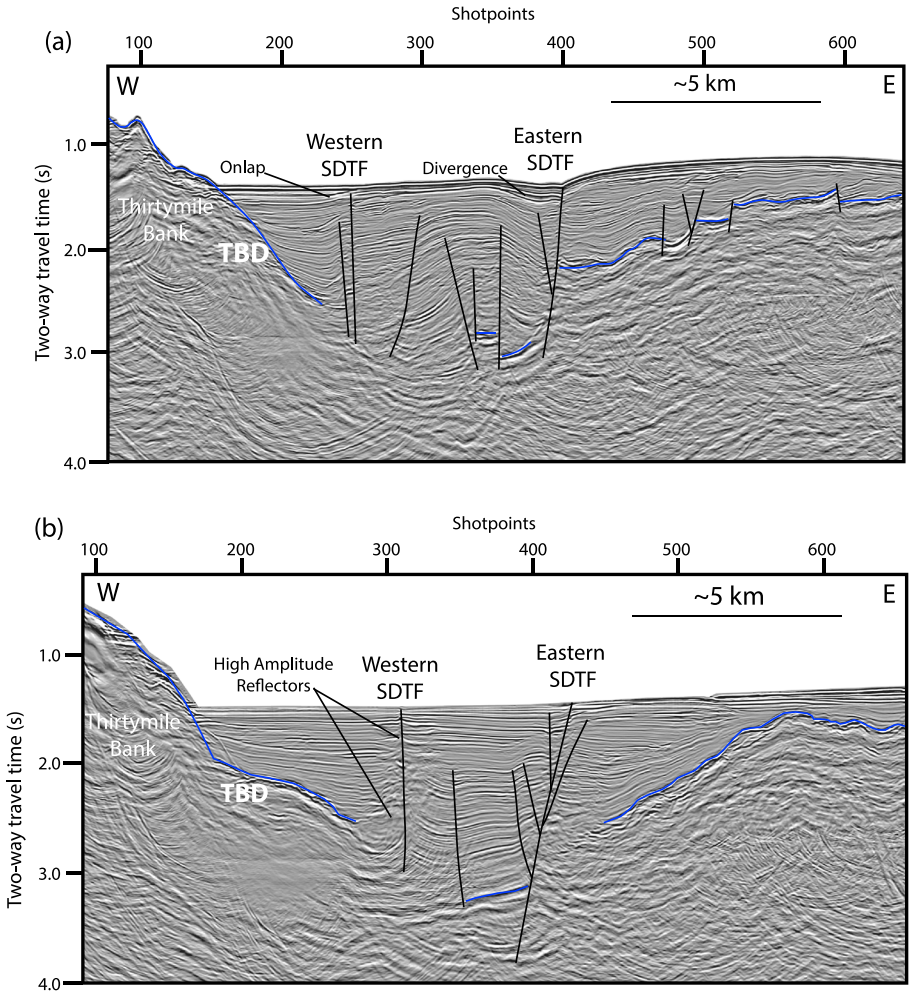

Figure 2. (a) MCS profile 4540 across the San Diego Trough, through the Del Mar Seep area. Blue horizon shows interpreted basement. Faults are marked as black solid lines. Location of the profile is shown in Figure 1a. (b) MCS profile 4544 located just to the south of the Del Mar Seep. The interpreted basement is shown in blue, and faults are drawn in black solid lines. See text for detailed description and interpretation. TBD = Thirtymile Bank Detachment.

frequency of 12 kHz, and Chirp data were collected with the hull-mounted Knudsen 3.5 kHz subbottom echosounder. Data were processed and interpreted using the following software packages: Caris Hips and Sips, IVS Fledermaus, ArcGIS, sioseis, and Kingdom Suite. A nominal 1500 m/s sound velocity was used to convert traveltime to depth for all Chirp data, and the resolution of these data is ~1 m. Reprocessed 1979 Chevron multichannel seismic (MCS) data (H-17-79 and H-18-79) were also examined to identify deep structures and fluid flow pathways associated with the seep (Figure 2) (see *Maloney* [2013] for methods).

Three site surveys were conducted with the ROV *Trident*. The ROV was navigated using Tracklink software, and locations are accurate within ~25 m. ROV video was examined, and general habitat zones were identified and mapped by linking time stamped images with navigation files. A 4.5 cm diameter push core was deployed with the manipulator arm and recovered ~7 vertical cm of homogenized sediment from a region of active gas seepage where an orange microbial mat covered the sediment surface. Geochemical and microbiological analyses were performed on the homogenized material. A multicorer also was deployed to collect sediment cores from three locations near the seep site (Figure 3). These multicores were sampled for macrofaunal abundance (see *Grupe et al.* [2015] for detailed biological methods and data).

The two multicores that collected sediment ~32 m from the seep (locations C_{32} in Figure 3) and the ROV push core were processed shipboard for geochemical analysis including alkalinity, methane, and dissolved inorganic carbon (DIC). The multicores were sectioned at a 3 cm resolution. Pore water was collected in

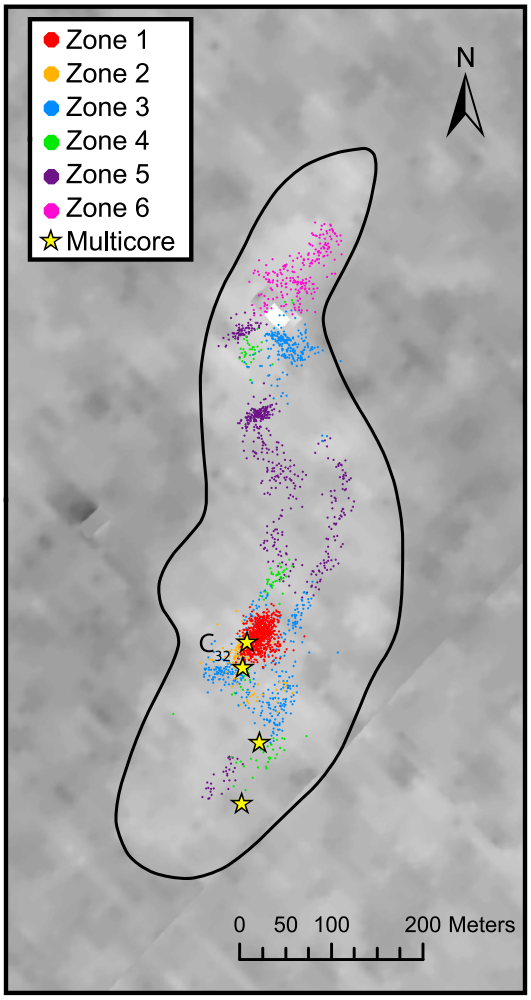

Figure 3. Enlarged view of the Del Mar Seep and the western region (WS) backscatter data with results from the ROV video survey and multicore locations overlain. See Figure 1c for location and inset legend for identification of ecological zones. A description of each zone is detailed in the text. The black line delineates the high backscatter zone. The two closely spaced multicore locations nearest to Zone 1 are considered as one location (C_{32}). The push core was taken within the Zone 1 area but is not plotted due to uncertainty in the ROV navigation system.

disposable syringes using a Reeburgh style squeezer under N_2. Prior to pore water collection, 3 mL of sediment was transferred to vials with 2 mL of 5 M NaOH; vials were capped with butyl rubber stoppers and crimped shut with aluminum seals for onshore methane analysis. Methane concentrations were determined from the average of triplicate measurements by gas chromatography flame ionization detection at the Caltech Environmental Analysis Center. The carbon and hydrogen isotopic composition of the methane was measured at the University of California (UC) Davis Stable Isotope Facility for the push core and the 7–10 cm horizon of a multicore from location C_{32} from the active seep area (Figure 3). Samples for DIC were passed through 0.2 μm syringe filters into He flushed 12 mL Exetainer vials (Labco Ltd., UK) with 100 μL 40% phosphoric acid. DIC concentration and carbon isotope composition were measured using a Gasbench II system interfaced to a ThermoScientific Delta V Plus isotope ratio mass spectrometer (ThermoScientific, Bremen, DE) as described previously by *Torres et al.* [2005]. Errors are reported as standard deviation for both concentration and isotope measurements.

3. Results

3.1. Geophysical Data

Geophysical evidence for the Del Mar Seep was identified in backscatter and Chirp data (Figure 1). Two areas of high backscatter correspond to areas of acoustic wipeout in the subbottom Chirp data (Figures 1b and 1c). These areas, located ~50 km off Del Mar, California, are herein referred to as the eastern and western regions of the Del Mar Seep. For both the eastern and western regions, the area of high backscatter is ~0.15 km^2. The eastern region is located near the crest of an anticline, and the western region is located ~1200 m downdip to the southwest (Figure 1c). The anticline is ~3.7 km wide along the profile shown in Figure 1c. Both areas appear to be associated with faulting (Figure 1c). At the western region, the seafloor is offset down to the southwest by a fault and horizon offset increases with depth. At the eastern region, we observe folding and faulting, but discrete offset of horizons is difficult to detect due to the acoustic wipeout.

Reprocessed Chevron MCS data image deeper structure across the San Diego Trough near the location of the seep (Figure 2). At the latitude of the seep, several strands of the SDTF offset acoustic basement, and we observe folding between the eastern and western strands (Figure 2a). The eastern strand appears to reach very near the seafloor, and reflectors to the west diverge toward the fault. The folding generates bathymetric relief and shallow reflectors onlap the anticline to the west of the western SDTF. In a profile just to the south of the seep, we observe high-amplitude reflectors at the western SDTF strand (Figure 2b). The high-amplitude reflectors are not observed in adjacent industry profiles to the north (Figure 2a). In the southern profile, there is less contractional folding and the eastern SDTF strand is imaged as a positive flower structure (Figure 2b). However, in the shallowest horizons west of the eastern SDTF, there is a slight

divergence toward the eastern SDTF. Near the latitude of the seep, we observe straight, lateral onlap onto the Thirtymile Bank detachment in the uppermost acoustic horizons. Deeper horizons between Thirtymile Bank and the western SDTF are characterized by dip to the east from the Thirtymile Bank detachment and slight synclinal folding just west of the SDTF strand.

3.2. Biological Data

An ROV survey of the eastern region revealed areas of carbonate rubble and sparse vesicomyid clam beds. Characteristics of active seepage, such as dense clam beds, extensive bacterial mats, or active venting, were not observed. An ROV survey of the western region (completed over two dives), however, revealed several habitats that exhibited zonation of visible substrate and associated benthic communities. Zone 1 included the center of seep activity where thick orange, yellow, and white bacterial mats, dense clam beds, complex carbonate structures, and gas bubbles actively venting from the seafloor were observed. Vesicomyid clam beds dominated the seafloor in Zone 2, which was restricted to an area within 5–10 m of Zone 1. In Zone 3, clam bed patches were observed at high density and faint white microbial mats were also identified. In Zone 4, there were low densities of clam patches and some patches of slight sediment discoloration. Whelks, burrows in the soft sediment, *Bathysiphon* (foraminifera) tubes, and isolated, single clams were observed in Zone 5. Zone 6 was also covered with soft sediment, but ophiuroids visually dominated the fauna. The extent of these zones for the area covered by the ROV surveys is mapped in Figure 3.

Two live vesicomyid clams (~8 cm length) were collected with the ROV and appeared similar to those observed in ROV video. Additional fauna collected via ROV or multicorer that are characteristic of methane seeps included the frenulate *Siboglinum veleronis*, the vestimentiferan tube worms *Escarpia spicata* and *Lamellibrachia barhami*, a smaller vesicomyid clam species (3 cm length), filamentous bacteria, dorvilleid and ampharetid polychaetes, the gastropod *Provanna laevis*, and folliculinid ciliates. *S. veleronis* and the small vesicomyid collected from the multicores had $\delta^{13}C$ values in the range of −33.5‰ to −40.0‰. A detailed description of macrofauna and microhabitats from the most active areas of the seep is given in *Grupe et al*. [2015].

3.3. Geochemistry Data

Geochemistry data were analyzed from cores near the western region of the Del Mar Seep. Pore water geochemistry profiles obtained from a push core within a microbial mat in the active seep area and from two multicores in a less active region on the edge of the seep (C_{32}, Figure 3) were compared. The push core from the microbial mat revealed an elevated methane concentration, 72.8 ± 3.1 μM, compared to the less active region, 18–36 μM (average 26.0 ± 7.2 μM). Methane in both active and inactive regions appeared to share a common source based on values for $\delta^{13}C_{CH4}$ (−59.9 ± 0.7‰) and δD (−184.8 ± 2.0‰). The alkalinity and DIC concentrations in the active seep core (Alk_{seep} = 4.5 mM; DIC_{seep} = 1.6 mM) were greater than those observed in the inactive region ($Alk_{off\text{-}seep\text{-}avg}$ = 2.7 ± 0.23 mM; $DIC_{off\text{-}seep\text{-}avg}$ = 0.37 ± 0.09 mM). Additionally, $\delta^{13}C_{DIC}$ indicated a ^{13}C-depleted source of carbon for respiration in both the active seep, (−33.0 ± 0.2‰) and at depth in the inactive region (−13.0 0 ± 0.4‰). Near the western region of the Del Mar Seep, a methane sensor (CONTROS Hydro™ CH4 Sensor, http://www.contros.eu/hydroc-ch4-hydrocarbon-methane-sensor.html) towed ~80 m off the seafloor indicated elevated methane concentrations (2–3 times background levels of methane) (S. Constable, personal communication, 2012). Due to a calibration problem, absolute methane concentrations were not available.

4. Discussion and Conclusions

The geology controlling fluid expulsion at the Del Mar Seep appears related to faulting and compression at a restraining step in the SDTF (Figure 1). This type of localized control on fluid seepage at the seafloor in strike-slip settings has yet to be fully investigated. We suggest that along transform fault systems, segment boundaries may play an important role in the distribution of fluid expulsion sites and associated seep habitat distribution. Seeps have been found associated with other strike-slip fault systems, but patterns in their distribution are not well understood. For example, in the Sea of Marmara, seeps are located along the North Anatolian Fault zone but are unevenly distributed along strike [*Zitter et al*., 2008; *Geli et al*., 2008; *Tryon et al*., 2012]. Nevertheless, variable tectonic structures along the North Anatolian Fault do appear to

exert some control on seep distribution and on characteristics of expelled fluids [*Tryon et al*., 2010a], with primarily shallow sourced, brackish, Pleistocene Lake Marmara fluids expelled along basin-bounding faults and deep sourced fluids expelled at topographic highs. Transform margins are characterized by localized zones of transpression and transtension associated with fault bends and steps that generate tectonic features along strike and may influence spatial patterns and distribution of fluid expulsion. In contrast, along convergent margins, tectonic forces generate regional compression and associated dewatering from deep fluid sources resulting in the distribution of seeps along the outer fore arc [e.g., *Tryon et al*., 2010b].

At the Del Mar Seep, we interpret the eastern region to be relatively inactive as indicated by disarticulated, sparse clam shells, carbonate rubble, and lack of microbial mats or active gas venting. The amount of carbonate rubble observed in ROV video suggests that this was at one time an area of active fluid expulsion. Faulting at the crest of the anticline appears to have created a conduit for gas migration. Additionally, the anticline would tend to focus fluid migration toward the crest, as is commonly observed in hydrocarbon traps [e.g., *Biddle and Wielchowsky*, 1994]. The site may no longer be active due to capping by authigenic carbonates (evidence from observed rubble), source depletion, or complex fault-fluid interactions [e.g., *Antonioli et al*., 2005; *Johnson et al*., 2000]. The wipeout in the chirp data indicates that gas may still be present in the sediments below the seafloor (Figure 1c). Given recent research on seep carbonates that indicates considerable microbial activity may persist without visible evidence of seep biota [*Marlow et al*., 2014], we suggest that additional ROV exploration may yet reveal chemosynthetic communities at this site.

The western region of the Del Mar Seep is currently an active methane seep with a small zone of focused fluid flow surrounded by areas of potentially diffuse flow. Active venting and extensive, thick microbial mats were observed only in a small area (~1200 m^2) in the southern part of the western region (Zone 1, Figure 3). The observed patchwork of biological zones on the seafloor may reflect a biological response to spatially and temporally varying flow. The seep is located along an active fault that vertically offsets the seafloor and appears to record previous events downsection, as evidenced by the increased offset of reflectors with depth (Figure 1c). The surface trace of the fault is confined to the area of the acoustic wipeout in Chirp data (Figure 1b). Additionally, the high-amplitude reflectors observed along the western strand of the SDTF in MCS data (Figure 2b) are indicative of fluid flow along the major fault strands near the Del Mar Seep.

Our geophysical data support the interpretation of this region as a localized pop-up structure along the strike-slip SDTF [*Ryan et al*., 2012]. SDTF strands are steep and exhibit variability with depth between transpressional deformation (flower structures) and transtensional deformation (diverging reflectors toward the fault). Additionally, lateral onlap of horizons at Thirtymile Bank suggest a lack of regional compression [*Rivero and Shaw*, 2011]. Furthermore, contractional folding appears highly localized along the SDTF, decreasing to the north and south in MCS data (Figure 2). The faults shown in Figure 1 are from a regional database, and our detailed survey reveals more complexity with two dominant strands and smaller, less continuous splay faults. Folding and contractional deformation are predominately observed between the two dominant fault strands, which suggests that slip along the eastern branch is transferred to the western branch. A left jog along a right-lateral fault system generates compression and is consistent with the observed deformation (Figure 2a). If the deformation was due to a larger bend along the western fault segment, the deformation would be shifted to the west instead of between the fault segments.

In the ICB, both the Del Mar Seep investigated here, and seeps in the Santa Monica Basin investigated by *Hein et al*. [2006] and *Paull et al*. [2008] are located along restraining step overs in offshore faults. The Santa Monica Basin seeps are located at a left step in the San Pedro fault zone, and the subseafloor geology at both seep locations is characterized by localized folding and faulting, with prominent anticlinal structures rising up from the basin floor. At restraining bends and steps, increased tectonic compression and deformation can be highly localized and promote fluid migration to the seafloor compared to the surrounding area due to increased fluid pressures, formation of anticlines, and complex fault conduits [*Bray and Karig*, 1985; *Carson and Screaton*, 1998]. Therefore, in a strike-slip tectonic setting, local stress variations may promote or suppress fluid expulsion at the seafloor and control regional patterns of seep distribution. This differs from convergent margins where compression is regional, causing more widespread fluid expulsion.

While the Santa Monica Basin seeps and Del Mar seeps are both located at pop-up structures near the crests of anticlines, they differ morphologically in that the Santa Monica Basin seeps form mounds $>$10 m high.

The western region of the Del Mar seep rises only slightly (~2 m), but both the eastern and western regions are primarily distinguished by rough and pockmarked seafloor. The formation of the Santa Monica Basin mounds has been attributed to diapirs or mud volcanoes [*Hein et al*., 2006] or alternatively to expansion of subseafloor gas hydrates [*Paull et al*., 2008]. We did not sample hydrate in any cores and a bottom-simulating reflector was not observed in the seismic data, but in May 2013, pits and craters were observed on the seafloor [*Grupe et al*., 2015] that could be signs of subsurface hydrate. The difference in morphology between the Santa Monica Basin and Del Mar Seep could be related to rates of fluid flow, presence or absence of gas hydrate, or the size of the gas reservoir. We propose that the Del Mar Seep is formed from compression at the SDTF restraining step over yielding fluid migration toward the crest of the anticline with focused fluid flow toward the seafloor along faults and fractures.

Seeps have also been identified in the ICB along the right-lateral, strike-slip San Clemente fault zone in the San Clemente Basin [*Lonsdale*, 1979; *Torres et al*., 2002; *Hein et al*., 2007]. At the location of the seeps, there are insufficient geophysical data to identify a bend or a step over. Nevertheless, a vertical scarp of 50–75 m with back-tilted acoustic horizons was observed at the location of the seep, indicating localized dip-slip motion [*Lonsdale*, 1979]. Other localized controls on seeps in the ICB could be related to erosion [e.g., *Eichhubl et al*., 2000; *Naehr et al*., 2000; *Paull et al*., 2008] or deposition (e.g., increased sedimentation and differential loading at submarine fans). The Del Mar Seep, Santa Monica mounds, and San Clemente seeps are all adjacent to canyon-fan systems.

The complexity of fault geometry and fault segmentation patterns in the ICB could play a major role in the distribution of seep ecosystems and their connectivity to one another. At the Del Mar seep, the low $\delta^{13}C$ values of a siboglinid (frenulate) polychaete and vesicomyid clam indicate that both within and away from the active Zone 1, chemosynthetic production supports symbiont-bearing metazoans. These taxa are known to harbor sulfide-oxidizing symbionts, which likely have access to higher sulfide concentrations due to syntrophic methane-oxidizing archaea and sulfate-reducing bacteria associated with the seep [*Nauhaus et al*., 2002]. The combination of carbon and hydrogen isotopic data for methane obtained from the push core and multicores suggest a common source for the two regions. The isotope compositional range for the methane indicates a likely biogenic origin associated with microbial CO_2 reduction [*Whiticar*, 1999]. ROV video of bubbles venting from the seafloor and the 2–3 times background increase in methane in the water column above the seep indicate that at least occasionally, methane gas escapes seep sediments without being metabolized by microorganisms. On a subsequent ROV investigation of the western region of the Del Mar Seep in May 2013, *Grupe et al*. [2015] did not observe gas bubbles venting from the seafloor.

Isotope data from the Santa Monica Basin seeps also indicated a biogenic source of methane, but fossil radiocarbon ages suggested that the gas is sourced from a reservoir at depth [*Paull et al*., 2008]. *Paull et al*. [2008] also observed continuous gas venting from one of the mounds and measured methane concentrations $>4500\ \mu M$ in pore water samples, much higher than measured at the Del Mar Seep. Although both are located at restraining step overs, fluid flow dynamics may differ between the sites. Fluid flow dynamics could impact biological recruitment and ecological succession through time. The impact of these restraining step overs on the constancy and rates of fluid flow is not well understood and further investigations into the geochemistry, biology, and microbiology of the Del Mar Seep are warranted to gain a better understanding of the dynamics and ecological linkages among seeps of the southern California margin.

The patterns of seep distribution and fluid flow across the ICB, as controlled by the tectonic setting, may play an important role in structuring regional ecology. Methane seeps increase the heterogeneity of continental margin habitats and influence margin biodiversity, which are both important for ecosystem functions and have implications for resource management [*Snelgrove et al*., 2004; *Danovaro et al*., 2008; *Levin et al*., 2010]. Due to their metabolic activities, seep-associated bacteria and archaea have elevated rates of in situ primary production relative to the surrounding deep sea [*Fisher*, 1996]. They perform important and only partially understood roles in biogeochemical cycling and provide both food and habitat for dense animal assemblages, which contribute to regional biodiversity patterns along continental margins [*Levin*, 2005; *Cordes et al*., 2010]. There is growing evidence that methane seeps can provide critical nursery grounds and adult habitat for cephalopods, elasmobranchs, and commercially valuable fishes [*Grupe et al*., 2015, and references therein]. The eastern Pacific continental margin is dominated by convergent tectonics, but

in the latitudes from Baja to Mendocino, the tectonic setting is characterized by strike-slip faulting. This area is ecologically productive and is a hydrocarbon-producing region, but the controls on fluid migration and expulsion at the seafloor differ from convergent margins, which are characterized by extensive regional tectonic compaction and deep fluid sources. In the ICB, however, the location of seeps appears related to localized fault segmentation. The alternating tectonic setting from north to south along the eastern Pacific margin could have implications for the long-term evolution of these systems and other continental margin ecosystems.

Further investigation of seeps located at fault segment boundaries may elucidate spatial and temporal patterns of fluid migration and expulsion and how they impact patterns of regional productivity and biodiversity. Importantly, the location of these seeps in terms of depth and proximity to the oxygen minimum zone also impacts biological communities [*Levin et al*., 2010; *Grupe et al*., 2015], adding further complexity to distribution patterns and connectivity. These areas also are interesting in terms of understanding the relationship between seismic activity and fluid expulsion. The Del Mar Seep is located near the epicenter of the 1986 Oceanside earthquake and fluid appears to be migrating along an active fault. Fault segment boundaries have been shown to influence earthquake rupture nucleation, propagation, and termination [e.g., *Wesnousky*, 2006; *Oglesby and Mai*, 2012], and segment boundaries add complexity to the poorly understood relationship between seismicity and fluid migration. We also anticipate that multiple seeps remain undiscovered in the ICB and that their locations may be closely linked to tectonic structures, especially strike-slip restraining bends and steps.

Acknowledgments

Data used in this publication will be provided by the corresponding author upon request. This research was supported by a UC Ship Funds grant awarded to Christina A. Frieder and by donations from Patty and Rick Elkus, Julie Brown, and Steve Strachan. Funds to reprocess the multichannel seismic data were provided by Southern California Edison. The authors would like to thank the R/V *Melville* crew and scientific party of the San Diego Coastal Expedition, especially Monika Krach, Sigrid Katz, Adriana Garcia, Valerie Sahakian, Rachel Marcuson, Drew Cole, and Jay Turnbull.

The Editor thanks Rob Evans and Johanna Nevitt for their assistance in evaluating this paper.

References

Antonioli, A., D. Piccinini, L. Chiaraluce, and M. Cocco (2005), Fluid flow and seismicity pattern: Evidence from the 1997 Umbria-Marche (central Italy) seismic sequence, *Geophys. Res. Lett.*, *32*, L10311, doi:10.1029/2004GL022256.

Becker, T. W., J. L. Hardebeck, and G. Anderson (2005), Constraints on fault slip rates of the southern California plate boundary from GPS velocity and stress inversions, *Geophys. J. Int.*, *160*(2), 634–650, doi:10.1111/j.1365-246X.2004.02528.x.

Bennett, R. A., W. Rodi, and R. E. Reilinger (1996), Global positioning system constraints on fault slip rates in southern California and northern Baja, Mexico, *J. Geophys. Res.*, *101*(B10), 21,943–21,960, doi:10.1029/96JB02488.

Biddle, K. T., and C. C. Wielchowsky (1994), Hydrocarbon traps, *AAPG Mem.*, *60*, 219–235.

Boetius, A., and F. Wenzhofer (2013), Seafloor oxygen consumption fuelled by methane from cold seeps, *Nat. Geosci.*, *6*, 725–734, doi:10.1038/NGEO1926.

Bray, C. J., and D. E. Karig (1985), Porosity of sediments in accretionary prisms and some implications for dewatering processes, *J. Geophys. Res.*, *90*(B1), 768–778, doi:10.1029/JB090iB01p00768.

Carson, B., and E. J. Screaton (1998), Fluid flow in accretionary prisms: Evidence for focused, time-variable discharge, *Rev. Geophys.*, *36*(3), 329–351, doi:10.1029/97RG03633.

Cordes, E. E., M. R. Cunha, J. Galeron, C. Mora, K. O. Roy, M. Sibuet, S. Van Gaever, A. Vanreusel, and L. Levin (2010), The influence of geological, geochemical, and biogenic habitat heterogeneity on seep biodiversity, *Mar. Ecol.*, *31*, 51–65, doi:10.1111/j.1439-0485.2009.00334.x.

Danovaro, R., C. Gambi, A. Dell'Anno, C. Corinaldesi, S. Fraschetti, A. Vanreusel, M. Vincx, and A. J. Gooday (2008), Exponential decline of deep-sea ecosystem functioning linked to benthic biodiversity loss, *Curr. Biol.*, *18*(1), 1–8, doi:10.1016/j.cub.2007.11.056.

Eichhubl, P., H. G. Greene, T. Naehr, and N. Maher (2000), Structural control of fluid flow: Offshore fluid seepage in the Santa Barbara Basin, California, *J. Geochem. Explor.*, *69–70*, 545–549, doi:10.1016/S0375-6742(00)00107-2.

Fisher, C. R. (1996), Ecophysiology of primary production at deep-sea vents and seeps, in *Deep-Sea and Extreme Shallow-Water Habitats: Affinities and Adaptations*, edited by F. Uiblein, J. Ott, and M. Stachowtisch, pp. 313–336, Australian Academy of Sciences, Vienna.

Geli, L., et al. (2008), Gas emissions and active tectonics within the submerged section of the North Anatolian Fault zone in the Sea of Marmara, *Earth Planet. Sci. Lett.*, *274*, 34–39, doi:10.1016/j.epsl.2008.06.047.

Grupe, B. M., M. L. Krach, A. L. Pasulka, J. M. Maloney, L. A. Levin, and C. A. Frieder (2015), Methane seep ecosystem functions and services from a recently-discovered California seep, *Mar. Ecol.*, doi:10.1111/maec.12243.

Hein, J. R., W. R. Normark, B. R. McIntyre, T. D. Lorenson, and C. L. Powell II (2006), Methanogenic calcite, ^{13}C-depleted bivalve shells, and gas hydrate from a mud volcano offshore southern California, *Geology*, *34*, 109–112.

Hein, J. R., R. A. Zierenberg, J. B. Maynard, and M. D. Hannington (2007), Barite-forming environments along a rifted continental margin, Southern California Borderland, *Deep Sea Res., Part II*, *54*, 1327–1349, doi:10.1016/j.dsr2.2007.04.011.

Hovland, M., and A. G. Judd (1988), *Seabed Pockmarks and Seepages; Impact on Geology, Biology and the Marine Environment*, Graham & Trotman, London.

Johnson, H. P., M. Hutnak, R. P. Dziak, C. G. Fox, I. Urcuyo, J. P. Cowen, J. Nabelek, and C. Fisher (2000), Earthquake-induced changes in a hydrothermal system on the Juan de Fuca mid-ocean ridge, *Nature*, *407*, 174–177, doi:10.1038/35025040.

Kulm, L. D., et al. (1986), Oregon subduction zone: Venting, fauna, and carbonates, *Science*, *231*, 561–566.

Le Pichon, X., K. Kobayashi, and K.-N. S. Crew (1992), Fluid venting activity within the eastern Nankai Trough accretionary wedge: A summary of the 1989 Kaiko-Nankai results, *Earth Planet. Sci. Lett.*, *109*, 303–318, doi:10.1016/0012-821X(92)90094-C.

Levin, L. A. (2005), Ecology of cold seep sediments: Interactions of fauna with flow, chemistry and microbes, *Oceanogr. Mar. Biol. An Ann. Rev.*, *43*, 1–46.

Levin, L. A., and G. F. Mendoza (2007), Community structure and nutrition of deep methane-seep macrobenthos from the North Pacific (Aleutian) Margin and the Gulf of Mexico (Florida Escarpment), *Mar. Ecol.*, *28*, 131–151.

Levin, L. A., G. F. Mendoza, J. P. Gonzalez, A. R. Thurber, and E. E. Cordes (2010), Diversity of bathyl macrofauna on the northeastern Pacific margin: The influence of methane seeps and oxygen minimum zones, *Mar. Ecol.*, *31*, 94–110, doi:10.1111/j.1439-0485.2009.00335.x.

Lonsdale, P. (1979), A deep-sea hydrothermal site on a strike-slip fault, *Nature*, *281*, 531–534, doi:10.1038/281531a0.
Maloney, J. M. (2013), Fault segments and step-overs: Implications for geohazards and biohabitats PhD dissertation, Univ. of California, San Diego, Calif.
Marlow, J. J., J. A. Steele, D. H. Case, S. A. Connon, L. A. Levin, and V. J. Orphan (2014), Microbial abundance and diversity patterns associated with sediments and carbonates from the methane seep environments of Hydrate Ridge, OR, *Front. Mar. Sci.*, *1*, 44, doi:10.3389/fmars.2014.00044.
Meade, B. J., and B. H. Hager (2005), Block models of crustal motion in southern California constrained by GPS measurements, *J. Geophys. Res.*, *110*, B03403, doi:10.1029/2004JB003209.
Moore, J. C., and P. Vrolijk (1992), Fluids in accretionary prisms, *Rev. Geophys.*, *30*(2), 113–135, doi:10.1029/92RG00201.
Naehr, T. H., D. S. Stakes, and W. S. Moore (2000), Mass wasting, ephemeral fluid flow, and barite deposition on the California continental margin, *Geology*, *28*(4), 315–318, doi:10.1130/0091-7613(2000)28.
Nauhaus, K., A. Boetius, M. Krüger, and F. Widdel (2002), In vitro demonstration of anaerobic oxidation of methane coupled to sulphate reduction in sediment from a marine gas hydrate area, *Environ. Microbiol.*, *4*, 296–305, doi:10.1046/j.1462-2920.2002.00299.x.
Oglesby, D. D., and P. Mai (2012), Fault geometry, rupture dynamics and ground motion from potential earthquakes on the North Anatolian Fault under the Sea of Marmara, *Geophys. J. Int.*, *188*(3), 1071–1087, doi:10.1111/j.1365-246X.2011.05289.x.
Paull, C. K., W. R. Normark, W. Ussler III, D. W. Caress, and R. Keaten (2008), Association among active seafloor deformation, mound formation, and gas hydrate growth and accumulation within the seafloor of the Santa Monica Basin, offshore California, *Mar. Geol.*, *250*, 258–275, doi:10.1016/j.margeo.2008.01.011.
Paull, C. K., A. J. T. Jull, L. J. Toolin, and T. Linick (1985), Stable isotope evidence for chemosynthesis in an abyssal seep community, *Nature*, *317*, 709–711.
Rivero, C., and J. H. Shaw (2011), Active folding and blind thrust faulting induced by basin inversion processes, inner California borderlands, in *Thrust Fault Related Folding*, *AAPG Mem.*, vol. 94, edited by J. H. Shaw and J. Suppe, pp. 187–214, AAPG, Tulsa, Okla.
Ryan, H. F., J. E. Conrad, C. K. Paull, and M. McGann (2012), Slip rate on the San Diego trough fault zone, inner California Borderland, and the 1986 Oceanside earthquake swarm revisited, *Bull. Seismol. Soc. Am.*, *102*(6), 2300–2312, doi:10.1785/0120110317.
Sahling, H., D. Rickert, R. W. Lee, P. Linke, and E. Suess (2002), Macrofaunal community structure and sulfide flux at gas hydrate deposits from the Cascadia convergent margin, NE Pacific, *Mar. Ecol. Prog. Ser.*, *231*, 121–138.
Silver, E., M. Kastner, A. Fisher, J. Morris, K. McIntosh, and D. Saffer (2000), Fluid flow paths in the Middle America Trench and Costa Rica margin, *Geology*, *28*(8), 679–682, doi:10.1130/0091-7613(2000)028<0679:FFPITM>2.3.CO;2.
Snelgrove, P. V. R., M. C. Austen, S. J. Hawkins, T. Iliffe, R. T. Kneib, L. A. Levin, J. M. Weslawski, R. B. Whitlatch, and J. R. Garey (2004), Ecosystem services provided by marine sedimentary biota and their vulnerability to anthropogenic disturbance, in *Sustaining Biodiversity and Ecosystem Services in Soils and Sediments*, edited by D. Wall, pp. 161–192, Island Press, Covelo, Calif.
Torres, M. E., J. McManus, and C. Huh (2002), Fluid seepage along the San Clemente Fault scarp: Basin-wide impact on barium cycling, *Earth Planet. Sci. Lett.*, *203*, 181–194, doi:10.1016/S0012-821X(02)00800-2.
Torres, M. E., A. C. Mix, and W. D. Rugh (2005), Precise δ^{13}C analysis of dissolved inorganic carbon in natural waters using automated headspace sampling and continuous-flow mass spectrometry, *Limnol. Oceanogr. Methods*, *3*, 349–360.
Tryon, M. D., C. G. Wheat, and D. R. Hilton (2010a), Fluid sources and pathways of the Costa Rica erosional convergent margin, *Geochem. Geophys. Geosyst.*, *11*, Q04S22, doi:10.1029/2009GC002818.
Tryon, M. D., P. Henry, M. N. Cagatay, T. A. C. Zitter, L. Geli, L. Gasperini, P. Burnard, S. Bourlange, and C. Grall (2010b), Pore fluid chemistry of the North Anatolian Fault zone in the Sea of Marmara: A diversity of sources and processes, *Geochem. Geophys. Geosyst.*, *11*, Q0AD03, doi:10.1029/2010GC003177.
Tryon, M. D., P. Henry, and D. R. Hilton (2012), Quantifying submarine fluid seep activity along the North Anatolian Fault zone in the Sea of Marmara, *Mar. Geol.*, *315–318*, 12–28, doi:10.1016/j.margeo.2012.05.004.
U.S. Geological Survey (2006), Quaternary fault and fold database for the United States. [Available at http//earthquakes.usgs.gov/regional/qfaults/, accessed 02/15/11.]
Wesnousky, S. G. (2006), Predicting the endpoints of earthquake ruptures, *Nature*, *444*, 358–360, doi:10.1038/nature05275.
Whiticar, M. J. (1999), Carbon and hydrogen isotope systematics of bacterial formation and oxidation of methane, *Chem. Geol.*, *161*, 291–314, doi:10.1016/S0009-2541(99)00092-3.
Zitter, T. A. C., et al. (2008), Cold seeps along the main Maramar Fault in the Sea of Marmara (Turkey), *Deep Sea Res., Part I*, *55*, 552–570, doi:10.1016/j.dsr.2008.01.002.

Erratum

In the originally published version of this article, the author affiliation of "California Institute of Technology, Pasadena, California, USA" was provided. This has been updated to "Division of Geological and Planetary Sciences, California Institute of Technology, Pasadena, California, USA". This version of the article may be considered the authoritative version of record.